TITLE: ENERGY DISPERSIVE SPECTROSCOPY USING SYNCHROTRON RADIATION: INTENSITY CONSIDERATIONS

AUTHOR(S): Earl F. Skelton, W. Timothy Elam, Syed B. Qadri, Alan W. Webb, David Schiferl

Los Alamos
Los Alamos National Laboratory
Los Alamos, New Mexico 87545

ENERGY DISPERSIVE SPECTROSCOPY USING
SYNCHROTRON RADIATION: INTENSITY CONSIDERATIONS

E. F. Skelton, W. T. Elam, S. B. Qadri and A. W. Webb

Naval Research Laboratory
Washington, DC 20375-5000, U.S.A

and

D. Schiferl

Los Alamos National Laboratory
Los Alamos, NM 87545, U.S.A.

Key words: X-ray diffraction; synchrotron radiation; energy dispersive x-ray intensities.

DISCLAIMER

Abstract

Detailed considerations are given to the reliability of energy dependent integrated intensity data collected from the pressure cavity of a diamond-anvil pressure cell illuminated with heterochromatic radiation from a synchrotron storage ring. It is demonstrated that at least in one run, the electron beam current cannot be used to correct for energy-intensity variations of the incident beam. Rather there appears to be an additional linear relationship between the decay of the synchrotron beam and the magnitude of the background intensity.

Introduction

Because synchrotron radiation (SR) is many orders of magnitude brighter than conventional x-ray tubes, it has proven to be a significant asset in the performance of x-ray scattering experiments which involve weak signals. Diffraction or fluorescence peaks can be weak because the sample is only available for brief periods of time, or because the sample volume is very small, or possibly a combination of these conditions. Recently it was demonstrated that x-ray structural data can be recorded in intervals as short as 50 ms. when SR is employed. This allows, inter alia, studying the kinetics of phase transformations which are completed in periods as short as 1 sec [1].

The high pressures which can be achieved in a diamond-anvil cell are in part due to the fact that the areas of the culet-faces of the diamonds are kept small, typically a few hundred micrometers in diameter. This of course results in a pressure cavity of microscopic dimensions, typically a volume of $1C^{-3}$ mm^3 and hence a comparatively small sample. Using a SR x-ray source and energy dispersive diffraction techniques, it has been demonstrated that the time required to collect structural information from a DAC can be significantly shortened [2,3]. Although it may be convenient to collect x-ray data relatively quickly from a DAC, there are some conditions under which it is essential. For example, recently an ultra-high temperature DAC has been designed and built which can be operated at temperatures in excess of 1500 K for brief periods of time [4]. A major difficulty operating a DAC at these thermal extremes is the

2

tendency of the diamonds to convert back to their thermodynamically stable form, graphite. This conversion can be inhibited for brief periods of time, if the DAC is heated in an oxygen free environment. However, the diamonds, like other components of this cell, have a limited life time at these temperatures and speedy collection of data is essential.

Experimental Procedure

In testing this ultra-high temperature DAC, it was first necessary to perform a series of temperature calibration measurements. These were accomplished by loading a Mo-13% Re gasket with a mixture of polycrystalline NaCl and Au. The cell temperature was measured with a W-5% Re: W-26% Re thermocouple mounted as close to the sample chamber as possible. Details of the design and operation of the cell are given in Ref. 4.

To correct for possible thermal gradients between the pressure chamber and the thermocouple, two calibration experiments were performed: (1) the melting of the elements Pb, Al, and Au was each observed visually and (2) the temperature was determined from the measured thermal expansion of Au. In this second method, energy dispersive x-ray diffraction (EDXD) spectra were recorded over a period of about 6-hours as the cell was heated to temperatures above 900K. Details of the EDXD measurement techniques are given in Ref. 5 and a typical EDXD spectrum is shown in Fig. 1.

Temperature calibration was achieved by comparing the measured thermal shift in the Au-(111) EDXD peak with that expected from the

thermal expansivity of Au, as reported by Kirby, Hahn, and Rothrock [6]. Based on this, the thermal expansion of NaCl was then determined from the measured shift in the NaCl (200) EDXD peak. These results are shown in Fig. 2 where the measured volume changes $(V(T)/V_o)$, are compared with the accepted values as determined from Ref. 6 (solid curve), using a reference temperature correction procedure to 20^oC similar to that detailed in Ref. 7. The experimental uncertainties in V/V_o are believed to be comparable to the size of the data points in Fig. 2. Clearly there is excellent agreement between the measured and accepted values of $V(T)/V_o$ for NaCl.

Intensity Considerations

Usually EDXD data collected with an SR source are used to measure compressibilities, or thermal expansivities or to detect phase transformations. In each case, it is the position, i.e. the energy, of the EDXD peak which is important. Changes in the crystal lattice are detected and measured by changes in the interatomic d-spacings through the Bragg relation

$$Ed \sin\theta = hc/2 \qquad\qquad (1)$$

where h is Planck's constant; c is the speed of light; θ is the diffraction angle; and E is the measured photon energy of the EDXD-peak. Thus, for cubic systems such as Au and NaCl, if the diffraction angle is held constant, fractional volume changes are simply the negative of thrice the measured fractional change in E.

However, the integrated intensities of EDXD peaks can also be used to determine crystallographic structures or to accelerate

4

evaluation of mean-squared atomic displacements through measurements of the Debye-Waller factors. The measured integrated intensity associated with the (hkl) EDXD peak from a polycrystalline sample at a temperature T can be expressed as follows:

$$\rho'(T) = I_o(E) \; A(E) \; W(E) \; \phi \; |F(hkl)|^2 e^{-2M(T)} (\nu E)^{-2} \tag{2}$$

where $I_o(E)$ is the SR intensity incident upon the sample at energy E, i.e. the intensity emerging from the storage ring, diminished by the attenuation from all absorbers in the beam path; W(E) is the efficiency of the detection system at energy E, A(E) is the absorption coefficient of the sample, plus everything in the path of the scattered beam; ϕ is the multiplicity factor; F(hkl) is the structure factor; $e^{-2M(T)}$ is the Debye-Waller factor at temperature T; and ν is the unit cell volume.

By considering ratios of measured intensities recorded at different temperatures, to that recorded at some arbitrary reference temperature, T_o, the temperature dependence of the mean-square atomic vibrational amplitudes, $\langle U^2(T)\rangle$, can be determined [8]. Conveniently, in considering these intensity ratios, most of the factors in eq. (2) cancel out, i.e., for a monatomic cubic material, such as Au,

$$\frac{\rho'(T)}{\rho'(T_o)} = \left[\frac{\exp \; -2\epsilon\langle U^2_{Au}(T)\rangle}{\exp \; -2\epsilon\langle U^2_{Au}(T_o)\rangle} \right] \tag{3}$$

or, for a diatomic cubic material crystallizing in the B1-structure, such as NaCl,

5

$$\frac{\rho'(T)}{\rho'(T_0)} = \left[\frac{\left| \mathcal{F}_{Na} \exp\left[-\epsilon <U_{Na}^2(T)> \right] + \delta_{hkl} \; \mathcal{F}_{Cl} \exp\left[-\epsilon <U_{Cl}^2(T)> \right] \right|^2}{\left| \mathcal{F}_{Na} \exp\left[-\epsilon <U_{Na}^2(T_0)> \right] + \delta_{hkl} \; \mathcal{F}_{Cl} \exp\left[-\epsilon <U_{Cl}^2(T_0)> \right] \right|^2} \right] \tag{4}$$

where $<U_x^2(T)>$, x=Au, Na, or Cl, is the mean-square displacement for each element; $\mathcal{F}_{Na}$ and $\mathcal{F}_{Cl}$ are the appropriate atomic scattering factors; δ is +1 for (hkl) all even and -1 for (hkl) all odd (mixed relections are forbidden in this space group); and ϵ is defined as follows:

$$\epsilon = \left[\frac{\pi \, E \, \sin\theta}{hc} \right] \tag{5}$$

In writing eqs. (3) and (4), we have neglected small differences in A(E) and W(E) which will arise due to the shift in E caused by thermal expansion.

In the Debye-Waller theory, the mean-square displacements can be expressed in terms of a Debye temperature, $\theta^M(T)$, through a weighted average over the lattice frequency spectrum, cf. Ref. 9 for details.

Comparison with Theory

The measured temperature dependence of the integrated intensities of the NaCl (200) and the Au (111) EDXD peaks are plotted in Fig. 3. The intensities have been normalized by dividing the area under the peaks by the beam current of the storage ring (SPEAR) as recorded at the beginning of each measurement. The data have also been corrected for background contributions. The mean statistical error in evaluating the peak intensity, defined as 100 times the square root of the area under the peak plus twice the background

6

intensity, divided by the area, is 0.27% and 1.61% for NaCl and Au, respectively. Thus, the uncertainty in the intensities due to statistics is less than the size of the symbols representing the data in Fig. 3.

The solid curve running through the NaCl data was calculated from the right-hand side of eq. (4) using the measured values of the Na and Cl Debye-Waller factors at 300K of Abrahams and Bernstein [10] and a linear extrapolation of the temperature dependence reported by Merisalo and Paakkari [11]. The solid curve running through the Au-data was calculated from the right hand side of eq. (3) using the accepted values for the Au Debye-Waller factors [12].

At first glance, comparison in Fig. 3 might be interpreted as reasonable agreement between the measured intensities of this work and previous studies. However, the excessive scatter in the data, especially in data below 500K is unreasonable and should be understood.

Eqs. (3) and (4) have been written from eq. (2) on the assumption that $I_0(E)$ is constant and therefore cancels out of each ratio. To further test this assumption, the temperature dependence of two fluorescence peaks, the Au L_β at 11.5 keV and the MoK$_\alpha$ at 17.5 keV, were also examined; these values are plotted in Fig. 4 and were also corrected for background contributions and normalized for changes in the SPEAR-beam current. The statistical uncertainty, defined in the same manner as above, is 0.83% and 0.73% for the Au and Mo peaks, respectively.

These fluorescence peaks involve relatively high energy level electronic transitions and should not exhibit any measurable tempera-

7

ture dependence in this thermal range, i.e. the structure and high temperature diminution seen in Fig. 4 are unreasonable.

A further measure of the apparent temperature dependence of the SR-beam intensities is provided by examining the background intensities. In Fig. 5 the apparent temperature dependences of the normalized background intensities of five 2 keV-wide energy windows centered at 6.0, 15.5 22.0, 33.0 and 45.0 keV, are plotted. As in Fig. 4, these values should be invariant to changes in temperature.

The observed variation in SPEAR beam current as the temperature of the DAC was being increased is plotted in Fig. 6; also shown in this figure is the corresponding time dependence. Each of the 14 spectra used in this analysis was recorded for a period of 10 minutes during which time the SPEAR beam current was reasonably stable. As seen in Fig. 6 following the first measurement, there was a SPEAR fill resulting in a current increase from 31 to 105 ma. Thereafter, some intermittent turbulance in the beam trajectory caused a relatively rapid loss of orbiting electrons to a current of about 44 ma. After this the beam remained relatively stable and the current gradually decayed to about 36 ma. The point being that the structure seen in the data below 450K in Figs. 3, 4, and 5 is probably attributable at least in part, to the turbulance in the SPEAR electron orbit. However, the data above 450K in each case, Figs. 3, 4, and 5, also exhibit a clear temperature dependence. To assess this, a linear least squares fit was made to these background intensities in each of the five energy windows. There is a linear correlation between the magnitude of the apparent $d\bar{I}/dT$-function and the back-

8   $\frac{d\bar{I}}{dT}$

ground intensity. As represented in Fig. 7, the greater the background intensity, the greater the apparent fall off with temperature. This leads to the conclusion that normalization of the measured intensities cannot be adequately accomplished with the value of the SPEAR electron current, i.e., a larger normalization factor is required, one which increases linearly with the background intensity. Additional experiments are required to determine the complete form of this correction.

Finally notice should also be taken of other effects which can affect the EDXD peak intensities. An examination of the NaCl-(200) EDXD peaks at 479K and 526K reveals a 35% <u>increase</u>, despite the fact that the background intensity is decreasing. It is presumed that this effect is related to the microscopic sample dimensions, i.e. because of the volume of samples used in the DAC may typically be 10^{-3} mm^3, the necessary condition of powder diffractometry, that a large number of crystallites be randomly oriented in the incident beam, is not always met. This, coupled with problems of preferred orientation, arising from non-hydrostatic stress state, can lead to EDXD peaks of anomalous intensity. Since these factors can vary in the course of a series of pressure or temperature measurements, they can also affect the data. It is presumed that this is the explanation of the aforementioned 35% intensity increase. One method of dealing with this problem is the magnetic stirrer attachment detailed in Ref. 13.

Conclusions

It is demonstrated that, in one series of experiments using SR with high temperature DAC studies, the SR electron beam current cannot be used to account for the apparent variation of the beam energy-intensity incident upon the sample. Whereas, EDXD data collected with a DAC and SR source can be reliably used for studies of the crystalline lattice size e.g. thermal expansivities, compressibilities, or phase transformations, when considerations are being given to the measured EDXD intensities, special attention must also be focused on variations in the incident beam energy intensity profile and to the sample crystallite distribution.

References

[1].   J.D. Ayers, W.T. Elam, C.L. Vold, S.B. Qadri, E.F. Skelton, and A.W. Webb, Rev. Sci. Instrum. 56, (1985) 712.

[2].   E.F. Skelton, Phyics Today 37(9) (1984) 44.

[3].   E.F. Skelton, J.D. Ayers, W.T. Elam, T.L. Francavilla, C.L. Vold, A.W. Webb, S.A. Wolf, S.B. Qadri, M.H. Manghnani, L.C. Ming, J. Balogh, C.-Y. Huang, D. Schiferl, and R.C. Lacoe, High Temp.-High Press. 16, (1984) 527.

[4].   D. Schiferl, A.I. Katz, R.L. Mills, L.C. Schmidt, C. Vanderborgh, E.F. Skelton, W.T. Elam, A.W. Webb, S.B. Qadri, and M. Schaefer, "A Novel Instrument for High-Pressure Research at Ultra-High Temperatures," presented at this conference (1985). Paper P2.

[5].   E.F. Skelton, S.B. Qadri, A.W. Webb, C.W. Lee, and J.P. Kirkland, Rev. Sci. Instrum. 54, (1983) 403.

[6].   R.K. Kirby, T.A. Hahn, and B.D. Rothrock, in American Institute of Physics Handbook, 3rd edition, (McGraw Hill, New York, 1972) pp. 4-124 & -139.

[7].   L.C. Ming, M.H. Manghnani, J. Balogh, S.B. Qadri, E.F. Skelton, and J.C. Jamieson, J. Appl. Phys. 54, (1983) 4390.

[8].   E.F. Skelton, Acta Cryst. A32, (1976) 467.

[9].   R.W. James, "The Optical Principles of the Diffraction of X-Rays," G. Bell and Sons, Ltd., London (1948), Chapt. V.

[10].   S.C. Abrahams and J.L. Bernstein, Acta Cryst. 18, (1965) 926.

[11].   M. Merisalo and T. Paakkari, Acta Cryst. 23, (1967) 1107.

[12].   International Tables for X-Ray Crystallography Vol. III, Birmingham: Kynoch Press (1962), p. 237.

[13].   E.F. Skelton, W.T. Elam, A.W. Webb, and S.B. Qadri, "Magnetic Stirrer for Diamond-Anvil Cells," presented at this conference (1985), Paper PP4.

Figure Captions

Figure 1: EDXD spectrum of a mixture of polycrystalline NaCl and Au contained in a Mo-13% Re gasket recorded with a Si(Li) detector at a diffraction angle of 8.38° in 2θ.

Figure 2: Temperature dependence of the fractional volume change, $V(T)/V_o$, for NaCl as determined from the measured shift of the NaCl (200) EDXD peak (dots) and from Ref. 6 (solid curve).

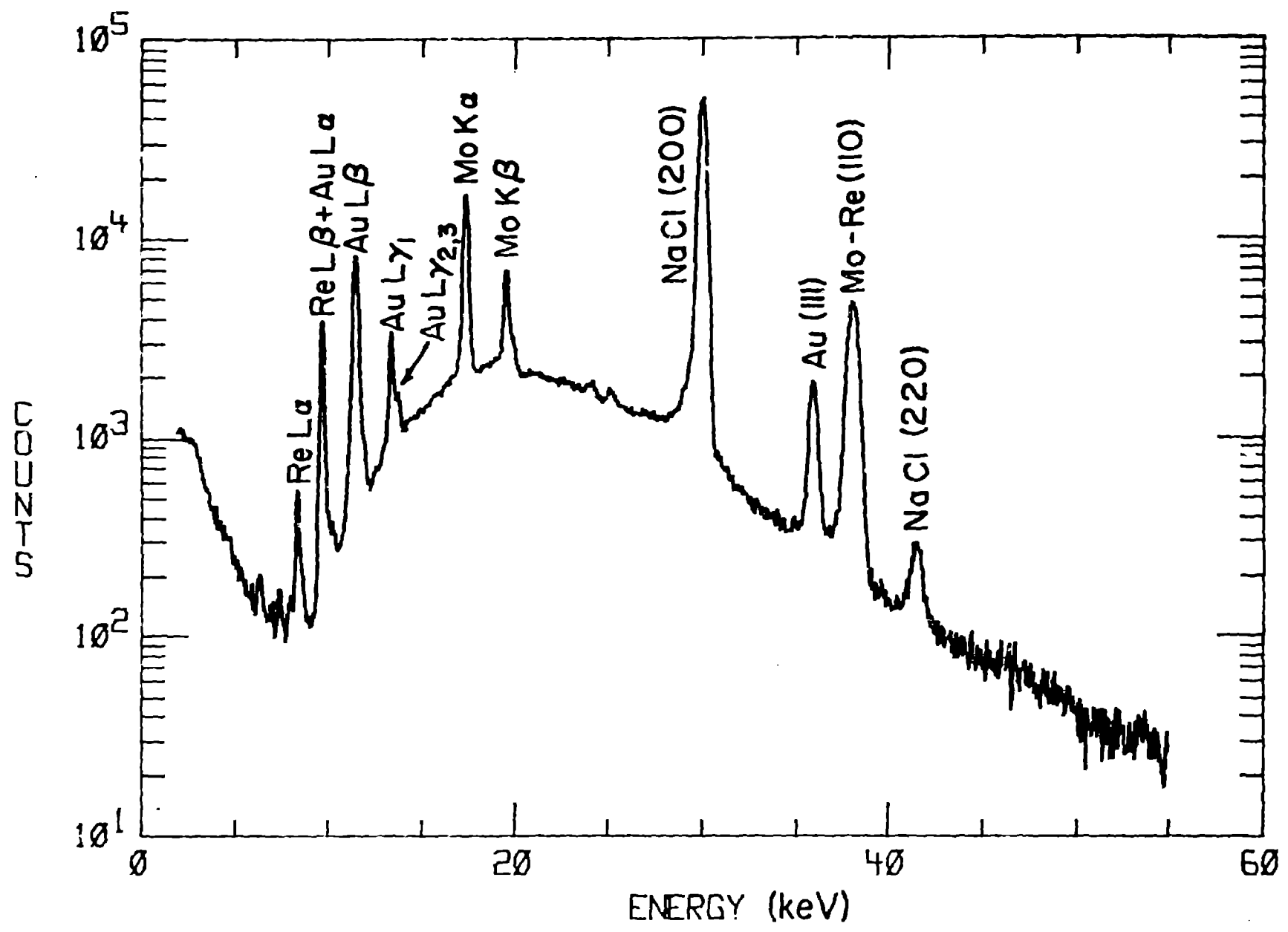Figure 3. Apparent temperature dependence of the measured, normalized integrated background corrected intensities of the NaCl (200) EDXD peak (squares) and of the Au (111) EDXD peak (circles); the solid curves are based on theory (see text).

Figure 4: Apparent temperature dependence of the measured normalized, integrated background corrected intensities of the MoK_α (squares) and the Au L_β (circles) fluorescence peaks.

Figure 5: Apparent temperature dependence of the measured, normalized background intensities in five 2 keV wide energy windows.
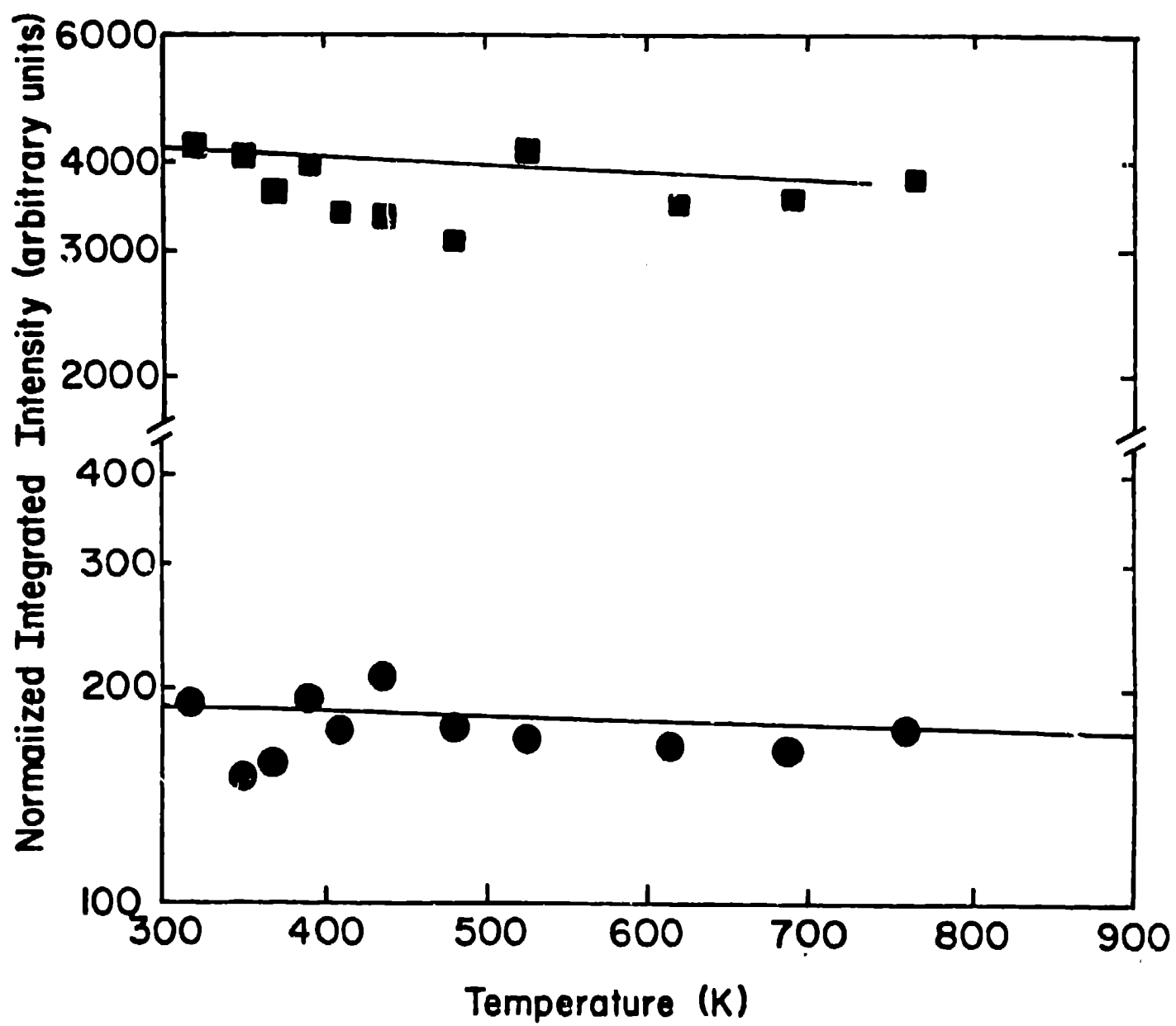
Figure 6: Apparent temperature dependence of the SR beam current. Data points were taken at the start of each 10-min. spectrum measurement; an approximate time dependence is also shown.
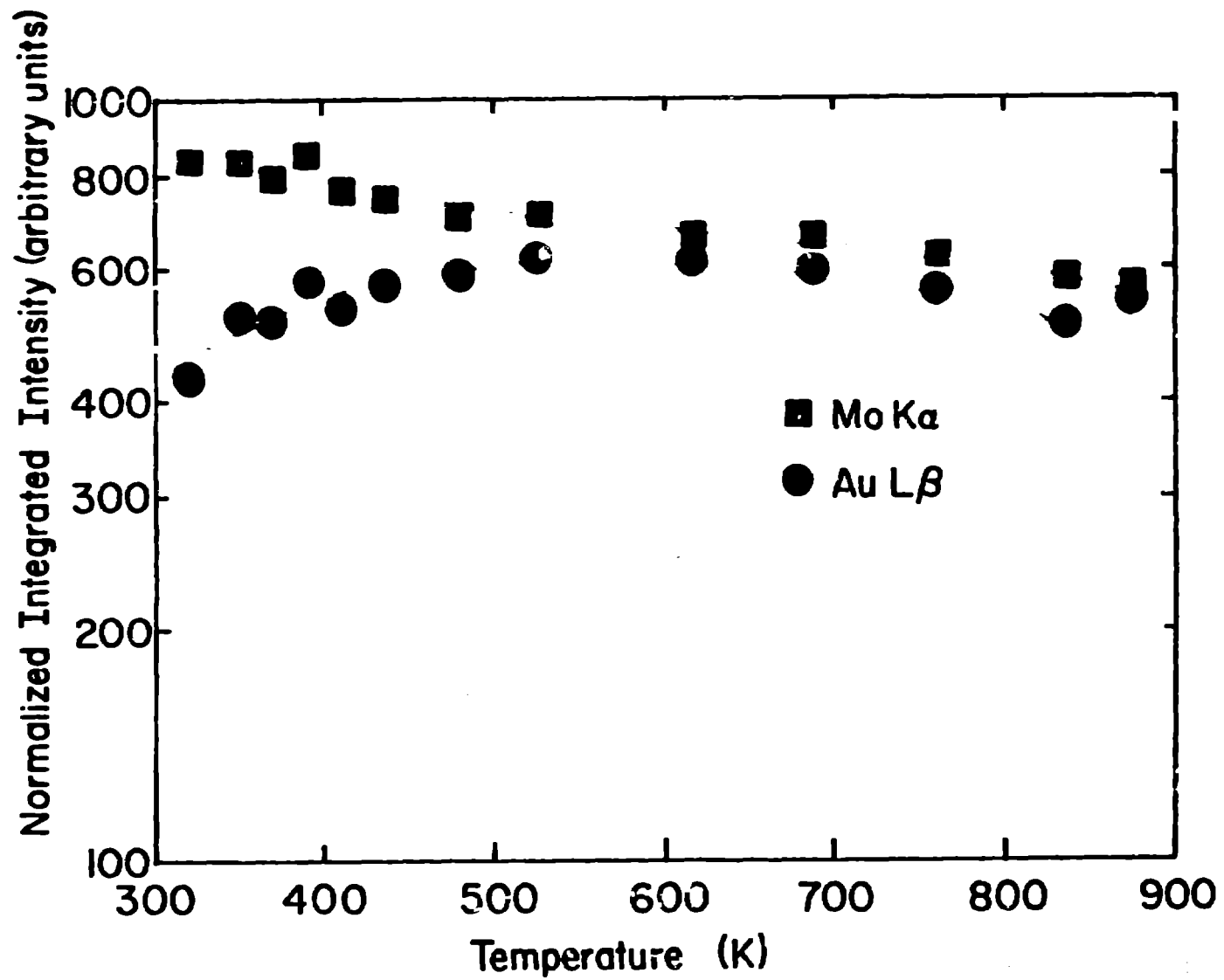
Figure 7: Intensity dependence of the apparent temperature dependence of the background intensity in each of five 2 keV energy window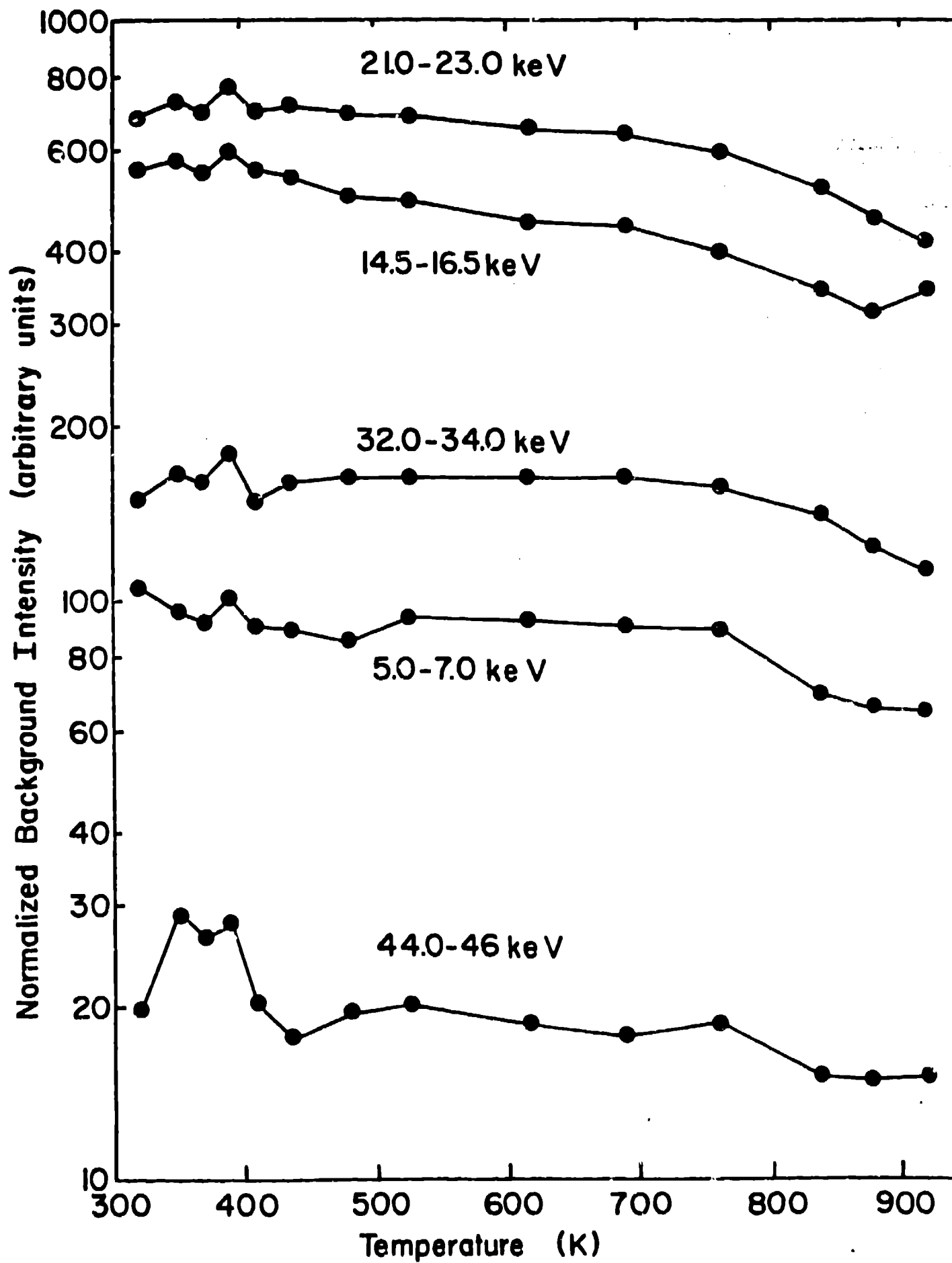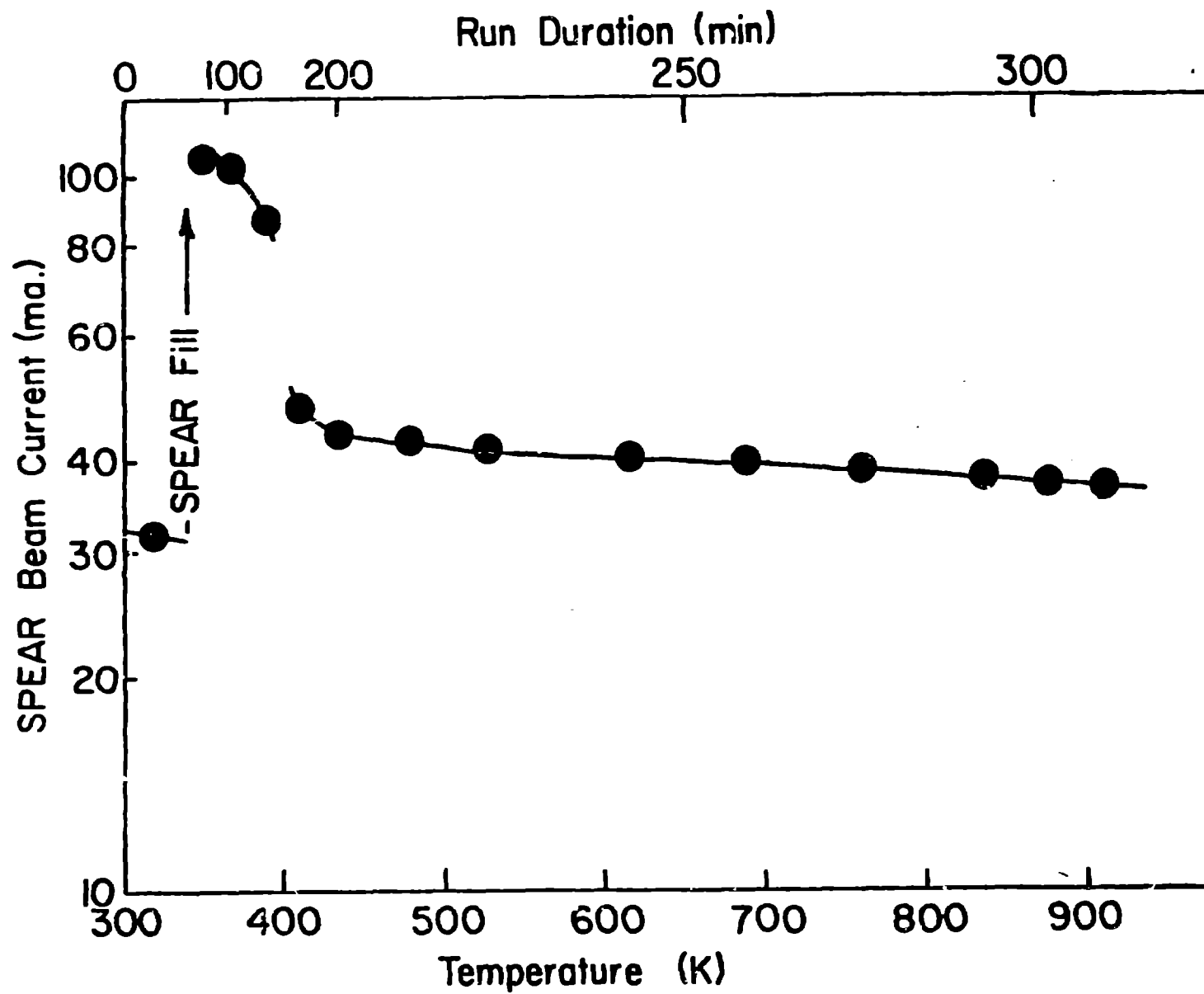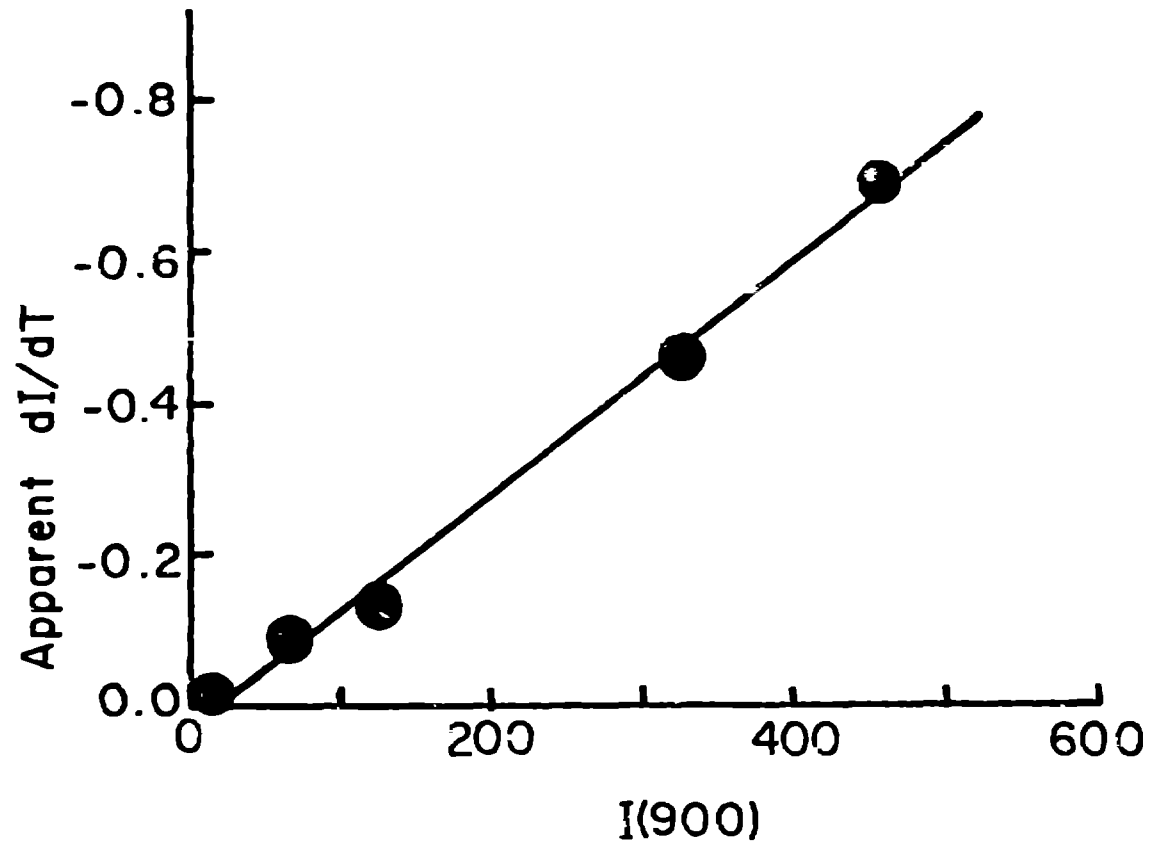s centered at 6.0, 15.5, 22.0, 33.0, and 45.0 keV.